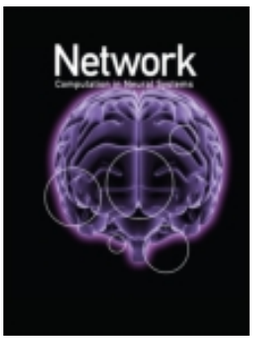

Network: Computation in Neural Systems

ISSN: 0954-898X (Print) 1361-6536 (Online) Journal homepage: http://www.tandfonline.com/loi/inet20

Cellular automaton models of the CA3 region of the hippocampus

E Pytte, G Grinstein & R D Traub

Network 2 (1991) 149–167 Printed in the UK

Cellular atuomaton models of the CA3 region of the hippocampus

E Pytte,†‡ G Grinstein† and R D Traub†

†T J Watson Research Center IBM Research Division PO Box 218 Yorktown Heights, NY 10598, USA

‡Almaden Research Center, IBM Research Division, 650 Harry Road, San Jose, CA 95120-6099, USA

Received 17 October 1990

Abstract. From the known properties of the hippocampal slice we have abstracted a cellular automaton model that incorporates many of the features of the CA3 region of the hippocampus, but which represents the neurons as binary variables The model is simple enough to allow efficient numerical simulation Results of simulations of a finite-size model with up to 10000 neurons, as well as the properties of the corresponding infinite-size limit, are shown to be in good agreement with the observed collective behaviour of hippocampal slices

1. Introduction

The subject of neural networks encompasses a broad range of research activities, from abstract studies of the mathematical properties of highly connected arrays of simple (typically binary) variables (see, for example, Amit 1989, Rumelhart *et al* 1988, and references listed therein) to detailed investigation of specific neurobiological systems whose basic elements — neurons — can be extremely complex. In the latter category, the mammalian hippocampus stands out as a particularly well characterized biological network Considerable data are available from *in vitro* studies on the properties of the neurons (for example, the morphology, membrane currents, and firing properties), and on the properties of the interactions between currents, and firing properties), and on the properties of the interactions between neurons, including the probability that a neuron of one type contacts a nearby neuron of any other type, and the different synaptic actions. (Chan-Palay and Köhler 1989, Frotscher *et al* 1988, Traub and Miles 1991) Indeed, the hippocampal slice is one of the few vertebrate systems for which it has been possible to obtain sufficient experimental information of this nature for the formulation of a realistic model Over the past decade, much of this knowledge has in fact been incorporated into a rather sophisticated and complex model, which contains a detailed description of the single neuron, with differential equations describing the different ionic currents, as well as a realistic representation of the known synaptic connectivity (Traub 1982, Miles *et al* 1988, Traub *et al* 1989) The model has been successful in reproducing some of the central features of the electrical activities measured in experiments on single neurons, as well as the observed properties of the entire network. It has been used both to explain existing experimental data and to make predictions subsequently verified by experiments. Given its attention to biological accuracy, it is not surprising that this model is computationally

0954-898X/91/020149 + 19$03 50

cumbersome For example, simulation of a network of 10000 neurons requires the numerical solution of roughly 250000 coupled differential equations

In this paper we attempt to reduce the essential structural features of this model as far as possible, while still retaining the global features The most drastic simplification we make is to replace the description of each individual neuron in terms of ionic currents and membrane potentials by a binary variable S which either fires ($S = 1$) or does not ($S = 0$) at every instant of time The model also evolves in discrete time steps, and the updating of the neurons is simultaneous It is therefore a cellular automaton (with interactions that are long-ranged in space), and so is similar in spirit to many of the diverse mathematical neural networks currently under investigation as paradigms for content-addressable memory, learning, and artificial intelligence However, the presence of interactions which extend over several hundred time steps distinguish it from many cellular automaton neural network models These memory effects enable the model to incorporate the rather long duration of the bursts of some neurons, refractoriness, and other complex behaviours of the real biological network This simplified model of the CA3 region is far easier to simulate numerically than its more realistic predecessor, and is even amenable to some analytic analysis The hope, therefore, is that it will prove a valuable tool in the continuing exploration of the behaviour and function of the hippocampus and of other types of cortex To be useful for this purpose it is essential that the model remain faithful to the underlying biological neuronal network. The main goal of this paper is to demonstrate that, insofar as we can judge, this is so despite the radical simplification of individual neurons, the model continues to represent accurately much of the known collective activity of the CA3 region of the hippocampus, producing results similar to those of the more realistic model It was not at all clear *a priori* that this would be the case Nor is it obvious that as more detailed experimental information about the hippocampus becomes available, binary neurons will continue to suffice Our idea is to continue to use binary variables until it proves impossible to account reasonably well for experimentally observed behaviour without restoring more internal structure to the neurons (Knowledge as to what can and cannot be accomplished with highly simplified neurons is presumably valuable in and of itself)

It is important to emphasize that, given the current incomplete knowledge of the function of the hippocampus, the diagnostics through which we judge the adequacy of the simplified model are necessarily primitive We rely for the most part on comparing the time dependence of the average activity of the network with that of the more realistic model and of hippocampal slices Within this limitation, however, the simplified model passes rather stringent tests For example, it reproduces not only the ordinary, low-amplitude chaotic oscillations of the *in vitro* CA3 region (Schneiderman 1986, Schwartzkroin and Haglund 1986, Miles and Wong 1987, Traub *et al* 1989), but the striking experimental observation of a sharp transition from these oscillations to fully synchronized firing as the strength of one type of inhibition is reduced (Miles and Wong 1987) At least as far as average activities are concerned, therefore, the model mimics the biology rather sensitively

The computationally efficient cellular automaton model is then available as a tool for study of the more intricate aspects of the network physics. As an example, we have calculated, for several parameter values in the low-amplitude, chaotically oscillating phase just discussed, the approximate time required for a small change in initial conditions (for example, changing the state of a single neuron) to propagate through the network The inverse of this time is a crude analogue for our discrete-variable network of the quantity, viz, the largest Lyapunov exponent, which measures the sensitivity to initial

conditions (see, for example Collet and Eckmann 1980) of continuous-variable systems such as coupled map lattices

In the hippocampus *in vitro*, the probability of two neurons being connected decreases with their spatial separation (Miles *et al* 1988) The decrease is sufficiently gradual, however (it occurs over a length scale of roughly 1 mm), that the 'infinite-range' approximation wherein the connection probability is independent of distance is believed to be a good one, at least for systems containing up to a few thousand cells It is also possible that the length scale is longer than 1 mm *in vivo* We have therefore incorporated infinite-range interactions in the cellular automaton model A feature of such long-range-interaction models familiar from statistical mechanics is that in the (thermodynamic) limit of an infinitely large system, one need only keep track of the average activity of each of the different types of dynamical variables — in this case neurons — to determine the collective properties of the system In this limit one can therefore solve most of the cellular automaton model analytically, reducing it to a set of 20 or so coupled map (or, more precisely, delay difference) equations with memory effects which extend over roughly 1000 time steps These equations are particularly easy to study numerically We find that this simple infinite-size model continues to reproduce faithfully the behaviour of its more detailed ancestors An interesting implication is that a system of, say, 1000 neurons is effectively at its thermodynamic limit, at least with respect to certain average behaviours we can detect little systematic discrepancy between the behaviour of the infinte-size model and the finite-size ones, provided that the latter contain on the order of 1000 neurons

Our starting point, the realistic model of the hippocampal slice, is a finite-size model with up to roughly 10000 neurons In section 2 we summarize the main biological facts that motivate and underpin this model Section 3 contains a description of our simplified cellular automaton version of it, while section 4 presents the numerical evidence for the legitimacy of this simplification, a qualitative explanation of the numerical results, and the calculation of the characteristic time which measures the sensitivity of the system to initial conditions In section 5 we outline the derivation of the infinite-size, coupled-map model, and show numerical data which indicate the similarity of its behaviour to that of its more detailed progenitors Section 6 presents a summary and discussion, while details of the construction of infinite-size models are contained in an appendix

2. The hippocampus and hippocampal slices

The hippocampus is anatomically the simplest type of cortex in the brain of mammals. The two hippocampi together constitute a relatively large part of the volume of the rodent brain, but a much smaller fraction of the human brain (Rodent and human hippocampi - specifically, the CA1 and CA3 regions together — each consist of roughly 6×10^5 and 7×10^6 neurons respectively (Boss *et al* 1987, Brown and Cassell 1980, Zola-Morgan *et al* 1986)) The hippocampi are essential for the formation of new 'single exposure' or 'declarative' memories, thus, in humans, it is not possible to learn new faces, the meaning of words, or new paths from one place to another, after bilateral hippocampal destruction (Squire *et al* 1989) Many of the cells in the rat hippocampus increase their firing rates when the animal is in some particular part of a larger environment (Eichenbaum and Cohen 1988, Muller *et al* 1987) Such cells are called place cells, and their discovery led to the proposal that the hippocampus registers a map of the environment (O'Keefe and Nadel 1978) Such a map, if it exists, cannot be hard-wired,

however, since the place-responsiveness of individual cells can be altered by moving a single object in the rat's environment (Muller and Kubie 1987) The cellular basis of these hippocampal functions is poorly understood One reason for the difficulty is that both memory and place-responsiveness involve diverse other parts of the brain, not just the hippocampus itself This is clear in the case of memory, since hippocampal destruction in humans leaves many old memories intact, so that they must 'reside' elsewhere (Scoville and Milner 1957) Similarly, place-responsiveness involves the processing of multimodal sensory information through many parts of the cortex before the hippocampus is reached

The hippocampus in rodents exhibits a number of EEG patterns, including theta rhythm (Green and Arduini 1954, Vanderwolf 1969, Buzsaki *et al* 1983) and physiological sharp waves (SPW) (Buzsáki 1986) These are interesting in part because of their close correlation with behavioural state For example, theta is recorded during walking and during REM sleep, while SPW are recorded during 'consummatory' behaviours such as drinking Theta waves appear in many interconnected brain structures, not just the hippocampus Indeed, the septal region can generate theta without the hippocampus, but the reverse is not true (Petsche *et al* 1962, Alonso *et al* 1987, Stewart and Fox 1989) In contrast, SPW appear to be generated within the CA3 region of the hippocampus itself, with subsequent spread to other regions (Buzsáki 1986) It is remarkable that the brain can switch between different collective modes (that is, EEG rhythms) depending on what the animal is doing One possibility is that release of slow-acting neurotransmitters serve to 'bring out' various collective modes by altering the intrinsic properties of the cells or synaptic interactions, an idea that has been documented in invertebrate central pattern generating circuits (Getting and Dekin 1985, Heinzel 1988a,b, Heinzel and Selverston 1988)

The hippocampus is important in clinical medicine, not just because of amnestic disorders, but for two additional related reasons First is its low threshold for initiation of epileptic seizures (Gastaut 1970) Second is its susceptibility to hypoxic/ischemic damage (Kass and Lipton 1982) and to cell loss caused by sustained seizures themselves (Sloviter 1983) Excitotoxic damage (cell loss caused by excessive release of excitatory neurotransmitter) may be the link between hypoxia- and seizure-induced lesions (Meldrum *et al* 1987, Olney *et al* 1986). Damaged hippocampus itself, for reasons not entirely clear, can then initiate — or contribute to the initiation of — *spontaneous* seizures (that is, be responsible for clinical epilepsy), in addition to having a low threshold for electrically induced seizures

It is important to have a better understanding of these aspects of normal and pathological hippocampal function However, the large number of cells that participate *in vivo* in any type of interesting behaviour has made progress difficult. In addition, it is technically hard to characterize *in vivo* the responses of single cells and the synaptic relations between cells The rat or guinea pig hippocampal slice preparation, containing 'only' thousands of cells, offers one approach. Although many types of normal physiological behaviour do not exist in the slice (e g place-responsiveness), slices do exhibit spontaneous EEG waves and a variety of epileptiform behaviours (reviewed in Traub and Miles 1991) Furthermore, one can readily study the electrophysiology of single cells in slices and, by using dual intracellular recordings, one can characterize the synaptic interrelations. the diversity of unitary synaptic actions (what does one action potential in a cell of type A do to a connected cell of type B?), and the probability of synaptic connections between pairs of nearby cells (Miles and Wong 1984, 1986, 1987) Using data from the slice, supplemented with data from isolated neurons (Wong and

Prince 1981, Miles 1990), a detailed circuitry model of the CA3 region has been constructed (Miles *et al* 1988, Traub *et al* 1989) This model is faithful in terms of its structure, and is able to reproduce a range of collective phenomena observed in the slice

The basic principles of the realistic model are these Each neuron is represented by a number of interconnected compartments containing resistance and capacitance, so as to capture something of the spatial extent of the soma-dendritic membrane In some or all of the compartments are embedded ionic conductances which are voltage dependent and/or calcium dependent (Traub 1982) Synaptic inputs impinge on the appropriate region of cell membrane, and the unitary synaptic effects mimic, as far as possible, the magnitude, time course and other characteristics (reversal potential, etc) that are observed experimentally Traces of simulated membrane potential (spikes, slow calcium spikes, bursts, afterpotentials, and so on) appear realistic In this way, the 'input–output' functioning of the cells are represented reasonably The model contains three types of cells (*excitatory* pyramidal cells, and *inhibitory* cells mediating either 'fast' $GABA_A$ or 'slow' $GABA_B$ inhibition, where GABA (γ-aminobutyric acid) is the inhibitory neurotransmitter) The first two cell types are known to exist and there is good indirect evidence for the third type The model contains about as many cells (in reasonable proportions) as does the experimental preparation, and the probabilities of interconnections are determined by dual recordings to the extent possible Unfortunately, only data on mean probability are available, not on *conditional* connection probabilities

It is useful to compare model and experimental behaviours as a single parameter is varied We have chosen most often to vary the strength of $GABA_A$ synapses (Traub *et al* 1987a, b, Traub and Miles 1991). The corresponding experiments can be performed by washing a $GABA_A$-blocker such as picrotoxin slowly into the bath around the tissue (Miles and Wong 1987) A number of different 'phases' exist in both model and slice with reasonable correspondence between model and slice. When inhibition is in the normal range, population waves occur with a period of several hundred ms Few of the cells fire during any one wave, and the firing of individual cells is irregular. Nevertheless, all of the cells receive synaptic inputs (usually excitatory and inhibitory) during each wave As inhibition is reduced, the population waves increase rather abruptly in amplitude (that is, more cells fire during each wave) and decrease in frequency. With inhibition sufficiently reduced, all of the cells fire together for about 100 ms This is followed by silence for several seconds, until the cells again all fire together This particular activity resembles the interictal EEG spikes often recorded from patients with focal seizure disorders (Daly 1990). In the model, at least, population waves have interesting properties. They appear to be chaotic (Traub and Miles 1991). The composition of the waves (that is, which cells fire during which wave) is highly sensitive to noise, the time scale on which small perturbations propagate through hippocampal circuitry may provide a constraint on how computation could be done in the hippocampus. Finally, the composition of succeeding waves has no recognizable statistical regularity It is not known if this is an artifact of the network construction since we have no data on conditional connection probabilities, the connectivity of model networks is assumed to be either random or locally random

This network model is accurate but cumbersome for the analysis of important questions where we would like to examine long-time behaviour, many parameter changes, scale effects, synaptic modifications, and so on These problems have motivated us to search for a computationally simpler model which still can generate the appropriate types of collective behaviour Given that computational simplicity demands sacrifice of membrane channel kinetics, what are the essential features which should be retained?

Our starting assumptions are that the following model features are relevant
(1) Sufficiently many cells (of order a thousand or more) must be present, in reasonable proportions, and with correct connectivity statistics
(2) CA3 pyramidal cells have a distinctive firing pattern, called an intrinsic burst, so that if one cell is excited sufficiently it fires for tens of ms, followed by a long refractoriness (hundreds of ms or seconds) This means, in particular, that the single-cell dynamics includes a *range of time scales*
(3) There is also a range of time scales in synaptic actions, as illustrated by these examples a single pyramidal action potential may elicit an action potential in an inhibitory cell at latency only 2 5–5 ms (Miles 1990) but it is unlikely to cause an action potential in another pyramidal cell (Miles and Wong 1986, 1987) A pyramidal *burst*, however, can elicit a burst in a connected pyramidal cell with latency 10–30 ms (Miles and Wong 1987, Traub and Miles 1991). The difference in time scale results here because pyramidal cells have a higher firing threshold than inhibitory cells, and because unitary EPSPs (excitatory postsynaptic potentials) are smaller onto pyramidal (excitatory) cells than onto inhibitory cells A $GABA_A$ IPSP (inhibitory postsynaptic potential) has a brief latency (a few ms) and the underlying conductance relaxes with time constant of order 10 ms (Collingridge *et al* 1984) A $GABA_B$ IPSP, however, has a latency onset of tens of ms, peaks at about 200 ms, and relaxes with time constant greater than 100 ms (Hablitz and Thalmann 1987) The difference in time scales here results because the different types of GABA receptor are coupled to outward membrane currents via different intracellular mechanisms A model need not describe such mechanisms precisely, so long as the time scale is right, for example, in the cellular automaton model we represent the delayed onset of $GABA_A$ ('fast') and $GABA_B$ ('slow') inhibition as 'propagation delays' of these inhibitory signals through the network

In the remainder of this paper, we show that a computationally efficient cellular automaton model based on these ideas is able to reproduce the two phases of behaviour discussed above

3. Description of the cellular automaton model

The cellular automaton model of the hippocampal (CA3) network summarized above is constructed as follows The neurons are of three different types excitatory (e), fast inhibitory (f), and slow inhibitory (s), the state of the ith neuron at time step n is specified by the binary variable $S_i(n)$ which is 1 if the neuron is firing and 0 otherwise The numbers of neurons of each type are respectively denoted N_e, N_f, and N_s, the total number of neurons is N. Each e, f, and s neuron is connected (i e sends signals) to exactly z_e, z_f, or z_s other neurons, respectively Connections from a given neuron to other neurons in the network are made randomly, and are assumed to occur with equal probability, regardless of neuronal type or position Thus on average each neuron receives input signals from $(\Sigma_\alpha N_\alpha z_\alpha)/N$, where α is summed over e, f, and s types The strength of the bonds for the three different kinds of neurons are denoted K_e, K_f, and K_s, respectively A firing neuron of type α ($=$ e, f, s) sends an output signal of strength K_α to each of the neurons to which it is connected

As discussed above, 'fast' ($GABA_A$-mediated) and 'slow' ($GABA_B$-mediated) inhibition refer both to the *duration* of the inhibition produced by the firing in a given inhibitory neuron on the neurons to which it is connected, and to the *latency* to onset of the inhibition The latency period for the output of an excitatory neuron to affect an

inhibitory neuron (fast or slow) to which it is directly connected is chosen to be the fundamental unit of (discrete) time in the model (We think of this as the time delay required for the signal to propagate through the network between the two cells.) We make this choice because in the hippocampus this latency period is of the order of 2 ms, a time interval shorter than any of the other times that characterize the system. We take τ_D^e, τ_D^f, and τ_D^s respectively to denote the latency period or time delay, measured in this basic unit, for a signal to propagate from an excitatory, fast inhibitory, or slow inhibitory neuron to an excitatory neuron to which it is directly connected.

Each excitatory neuron fires by either of two distinct mechanisms: spontaneous or stimulated. It will fire spontaneously $(\tau_S + 1)$ time steps after the end of its last burst, regardless of the excitatory and inhibitory inputs it receives from other neurons at that time. A distribution of spontaneous firing times τ_S is used, the value of τ_S being fixed for each neuron. Alternatively, a neuron will be stimulated to fire by the input signals it receives, whenever the total strength of its excitatory inputs exceeds that of its inhibitory inputs by a preassigned threshold. The threshold condition for stimulated firing of an excitatory neuron depends on the number of time steps, n, since that neuron last burst, i.e.

$$m_e(n)K_e - (m_f(n)K_f + m_s(n)K_s) > h(n - \tau_R) \tag{1}$$

where $m_e(n)$, $m_f(n)$, and $m_s(n)$ are the numbers of inputs of the three types arriving at the neuron in question at time n, and τ_R is the refractory period of the neuron. For $n < \tau_R$, the threshold $h(n-\tau_R)$ decreases monotonically with n. Usually a simple linear dependence is used:

$$h(n - \tau_R) = \begin{cases} F_0(\tau_R - n)/\tau_R & n < \tau_R \\ 0 & n > \tau_R \end{cases} \tag{2}$$

where F_0 is a positive constant of order unity. Thus the threshold falls to zero for $n > \tau_R$. There is a distribution of refractory periods for τ_R similar to that for τ_S, the values of τ_R and τ_S for any given neuron are correlated, with $\tau_S > \tau_R$.

For the inhibitory neurons the firing condition is simply

$$m_i(n) > 0 \tag{3}$$

A single excitatory input will therefore trigger a burst in an inhibitory neuron independently of the number of inhibitory inputs. In the model, inhibitory neurons do not fire spontaneously. (Some spontaneous firing of inhibitory cells does occur in CA3, but whether this affects the network properties importantly is unknown.)

The length of time during which a firing burst in one neuron affects the firing in another to which it is connected differs significantly for the three neuronal types; these times are represented in the model by assigning different durations, denoted d_e, d_f, and d_s, respectively, to the bursts of e, f, and s neurons. In other words, once a neuron begins firing, it is taken to continue firing for some interval. This assumption is not precisely correct in the hippocampus, but it is the simplest approximation that allows us to summarize the different membrane potentials (e.g. intrinsic bursting) and different durations of synaptic actions, which together determine the influence one neuron exerts on another.

Typical numbers appropriate to the hippocampus are $z_e = 20$, $z_f = 200$, $z_s = 200$, $N_e = 0.9N$, $N_f = N_s = 0.05N$, where N is the total number of neurons. Thus while the number of excitatory neurons is much larger, the number of excitatory outputs per neuron is much smaller, such that the total numbers of excitatory and inhibitory

synapses are comparable. However, the inhibitory bond strengths are much larger than the excitatory bond strengths. Typically $K_e = 1.0$, while $K_f = K_s = 10$. A typical value of the parameter F_0 in the threshold function is $F_0 = 2.0$. Typical values of the propagation delay times are $\tau_D^e = 10$, $\tau_D^s = 25$ and $\tau_D^f = 1$ (no delay). Typical values for the duration of bursts are $d_e = 20$, $d_f = 20$, and $d_s = 100$. Thus, compared to fast inhibitory neurons, slow inhibitory neurons keep firing for many more time steps and send signals that 'propagate' more slowly, i.e. there is a longer delay between firing and onset of synaptic action. Typical values for the refractory period are 700–900 and for the spontaneous firing time 900–1200.

4. Simulation of the finite-size cellular automaton model

The model just described is easy to simulate on a computer. Having fixed the total number of neurons of each type, established the network of connections, and chosen the τ_R and τ_s for each excitatory neuron according to the above rules, one initializes all the neurons to zero, then starts the simulation by setting $S_i = 1$ for one or more of the excitatory neurons. All neurons are simultaneously updated at every subsequent time step, via the algorithm outlined above. The fraction, x, of neurons firing at each time n is recorded: $x(n) = N^{-1} \Sigma S_i(n)$.

Figure 1(*a*) shows the behaviour of $x(n)$ for $N = 900$ neurons, and the 'typical'

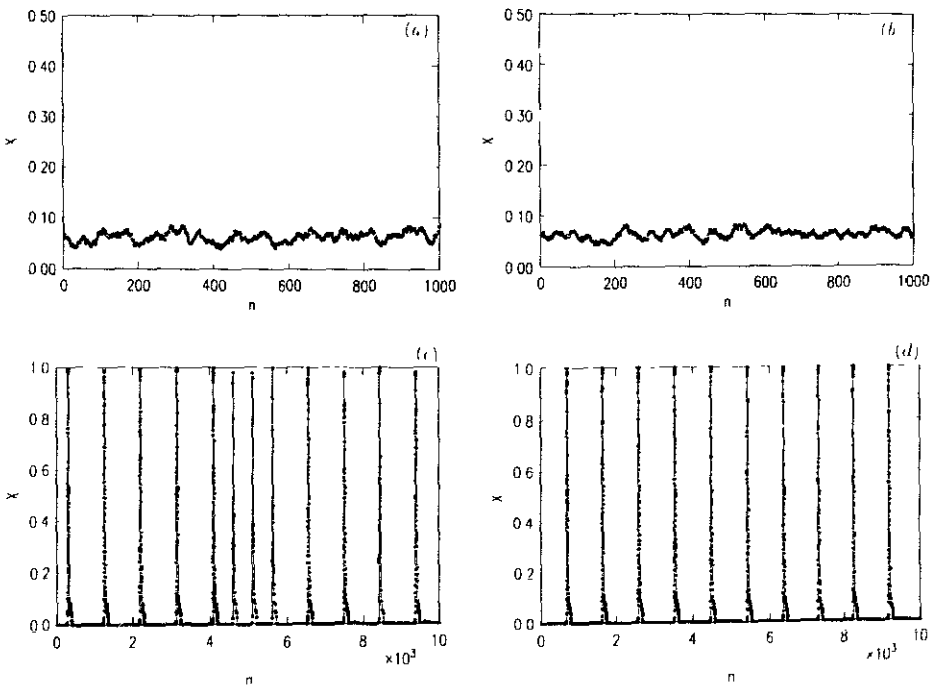

Figure 1. Fraction of neurons firing as a function of time for finite-size model with $N = 900$. The values of the parameters used are given in text. Only the strength of the fast inhibitory neurons is varied. (*a*) $K_f = 10$, (*b*) $K_f = 0.448\,88$, (*c*) $K_f = 0.448\,87$, (*d*) $K_f = 0$.

parameter values listed at the end of the previous section (Note that all of the figures have been generated by first letting the system run long enough so that all transient behaviour has disappeared.) The low-amplitude ($\sim 5\%$) chaotic oscillations are closely similar to those observed in hippocampal slices, and in the detailed model, under normal conditions This behaviour is observed in our model for a wide range of parameters. It resembles the population rhythm seen in CA3 *in vitro* during minimal blockade of $GABA_A$ inhibition (Miles and Wong 1987, Traub *et al* 1989). It is also reminiscent of the theta rhythm observed *in vivo*, in that the fraction of neurons firing during each wave is small, and in that the firing of the neurons (particularly inhibitory ones) is strongly correlated with the oscillation maxima (Buzsáki *et al* 1983). (It differs, however, from *in vivo* theta rhythm in two respects (1) bursting is rarely observed in CA3 pyramidal cells during walking theta (G Buzsáki, personal communication); (2) *in vivo* theta is apparently not intrinsic to CA3, but is rather dependent on inputs from other structures.)

As a more sensitive test of the cellular automaton model, we succeeded in reproducing the rather dramatic transition, observed in experiments wherein the strength of the fast inhibition in hippocampal slices is reduced chemically (Miles and Wong 1987) from the low-amplitude chaotic behaviour of $x(n)$ to sharply peaked, large-amplitude, nearly periodic (though still chaotic) oscillations. An example of these large amplitude oscillations is shown in figure 1(*d*), generated by setting $K_f = 0$ with all other parameters unchanged from figure 1(*a*). The transition itself is illustrated in figures 1(*b*) and (*c*), obtained from our model with $K_f = 0.448\,88$ and $K_f = 0.448\,87$, respectively (other parameters being held fixed). Figure 1(*b*) is closely similar to figure 1(*a*), whereas in figure 1(*c*) the peaks are much less regular than the very nearly periodic behaviour seen in figure 1(*d*) for $K_f = 0$. The transition is clearly very sharp, a feature characteristic of all the finite-size models we studied (All of these cases had $N \leqslant 10\,000$.) However, in the low-amplitude phase there are slow transients in the transition region. The time required to obtain the asymptotic, large-time behaviour in this phase increases markedly near the transition.

We now discuss the features of the model necessary for obtaining the range of behaviours illustrated in figure 1. Having the three different types of neurons and the different time delays is the first requirement: with K_f at 'full' strength ($K_f = K_s = 10K_e$), the inhibition is always too strong for a very large signal to be generated (figure 1(*a*)). As K_f is reduced, the excitatory inputs eventually become sufficient to overcome K_f in the threshold condition and a large signal has a chance to build up before the additional (slow) inhibitory inputs, delayed by τ_D^s, cut off the signal. That is, the combined effect of the K_f and K_s bonds ultimately becomes sufficient to overcome the excitation; large-amplitude oscillations (as in figure 1(*c*)) result. If the delay of the slow inhibitory neurons τ_D^s is set equal to that of the excitatory neurons, the low-amplitude phase is obtained for all values of K_f. In this case the inhibition is always too strong to allow a large signal to build up. This difference in delay time is, therefore, an important feature of the model. The relatively long duration of the slow inhibitory burst assures that the signal gets sharply reduced. In fact, for the parameters used in figure 1(*d*), it is reduced to zero between the spikes. If the duration of the burst for the slow inhibitory neuron is shortened so as to be equal to that of the excitatory and fast inhibitory neurons, a periodic sequence of sharp, large-amplitude peaks is obtained for all values of K_f. Thus the difference in the duration of the firing of the slow inhibitory neurons is also central to producing the observed behaviour.

While we get the large-amplitude phase for $K_f = 0$, $K_s = 10$ because of the propagation delay of the slow inhibitory neurons, setting $K_f = 10$, $K_s = 0$ yields the low-

amplitude chaotic phase In this case the (fast) inhibitory inputs are always too strong to allow a large signal to develop With both $K_f = 0$ and $K_s = 0$, all the neurons fire continuously, and the value of $x(n)$ saturates and remains at 1 0 For the choice of parameters $F_0 = 2\,0$ in the threshold function, slow inhibition is required to cut off the large-amplitude signals When F_0 is so large (i.e of order 10) that there is no firing of the excitatory neurons during the refractory period, however, we still obtain large peaks, separated by the spontaneous firing time, even for $K_f = 0$ In this case, though, the large signal is cut off by the refractory time and does not depend on the value of K_s By the time K_s can have an effect, the signal has already been attenuated by the refractoriness

It is known that the large-amplitude behaviour can be obtained with excitatory neurons only (Traub and Wong 1982, R D Traub, unpublished data) This can be obtained in our model by taking F_0/K_e sufficiently large, so that the signal is cut off by intrinsic refractoriness even in the absence of inhibition

It is also very important to have a distribution of spontaneous firing times in order to obtain the low-amplitude phase (figure 1(*a*)) If we used a single spontaneous firing time we found sharply spiked, periodic behaviour for all values of K_f, the period being determined by the spontaneous firing time In this case, a strong, synchronized burst is generated at the common spontaneous firing time On the other hand, whether we used a distribution of refractory times or just a single time made very little difference. The refractory period in this model is just the time, n, where the threshold function $h(n-\tau_R)$ goes to zero Thus a variation in τ_R from one neuron to the next does not significantly affect the results

Other features, such as the number of excitatory and inhibitory neurons and connections, are not critical at least so long as the total strength of excitatory and inhibitory signals remain nearly the same. Thus if instead of $z_e = 20$, $z_f = z_s = 200$ and $N_e = 0\,9\,N$ we use $z_e = z_f = z_s = 50$ and $N_e = 0.5\,N$, the results remain qualitatively the same. However, changing the number of connections changes the pattern of peaks in the high-amplitude phase at $K_f = 0$. Instead of a single uniformly spaced peak as, for example in figure 1(*d*), repeating patterns of several peaks (2, 3, 4 or 5, etc) can be obtained Also, for lower numbers of connections one gets a more gradual increase in the peaks with decreasing K_f, with an increasing separation of the peaks as their amplitude increases

In this section we have shown that a simple model which incorporates the different types of neurons of the hippocampus and the various time constants, but neglects almost all the internal degrees of freedom of the neurons, is able to reproduce much of the global behaviour observed in hippocampal slices and obtained in a more detailed model. To demonstrate the usefulness of this simplification for exploring the properties of the network, we have studied the sensitivity of the system to small changes in initial conditions, in the low-amplitude phase. In this study, the system is interrupted at some arbitrary time in its evolution, several sites are chosen at random and all of them are set to 1, any chosen site whose value is 0 is therefore altered by this perturbing operation Then the system is allowed to continue running without further external influence, and its subsequent time evolution compared with that of the unperturbed system Typical results are shown in figures 2(*a*) and 2(*b*), where the difference in the total fraction of neurons which fire in the perturbed and unperturbed systems is plotted as a function of time, n The results are largely independent of precisely how the perturbation was applied (e g. the number of spins initially perturbed, which precise spins were perturbed, etc). To generate figure 2, we applied the perturbing operation to ten arbitrarily chosen sites, and used the parameter values listed in the figure caption. The transition from the low- to the

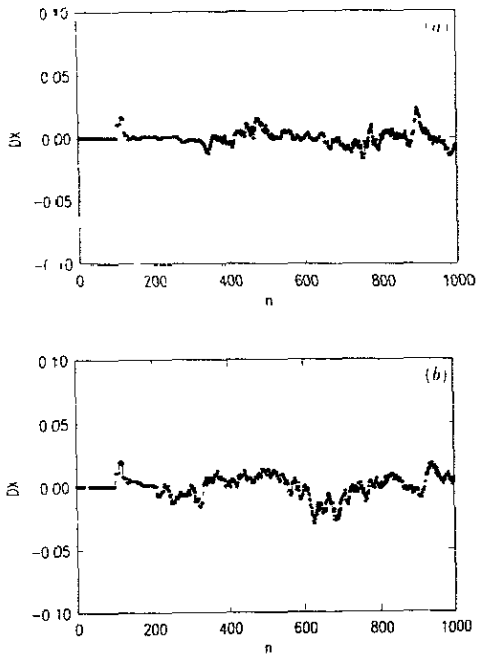

Figure 2. The change in $x(n)$ due to a perturbation applied to 10 spins at $n = 100$ for (*a*) $K_f = 10$ (*b*) $K_f = 2.8$ Values of the other parameters are as in figure 1, except $\tau_D^+ = 125$, $\tau_f = \tau_s = 100$, and τ_S, for which we used a uniform distribution of values between 1200 and 1800 For these parameters, the transition occurs for K_f between 2.4 and 2.5

high-amplitude phases for these parameters occurs at a value of K_f between 2.4 and 2.5. Thus figures 2(*a*) and 2(*b*) respectively correspond to parameters deep inside and close to the boundary of the low-amplitude phase As is clear from the figures, the initial perturbation was applied at $n = 100$ (after first running the system for 9000 time steps).

From each of the figures one can read fairly unambiguously the time required for the decorrelation of the perturbed system from the original one. These 'decorrelation times', whose inverses are crude analogues of the largest Lyapunov exponent (Collet and Eckmann 1980), which characterizes the chaotic state of extended dynamical systems with continuous variables, are roughly 200 and 100 time steps for $K_f = 10$ and $K_f = 2.8$, respectively. These results are somewhat surprising, given the fairly clear interpretation of the low-amplitude phase as 'more chaotic' than the high-amplitude one. Naively, therefore, one might expect the system to become progressively more chaotic, i.e. to have a shorter decorrelation time, as one moves deeper into the low-amplitude state. This, however, appears not to be the case. Since our goal here is merely to demonstrate the easy feasibility of such calculations (which are extremely laborious in the more realistic model) in the cellular automaton representation, we have not tried to study the details of the variation of the decorrelation time with K_f throughout the phase. Nor have we attempted to calculate this quantity in the high-amplitude phase, in part because, unlike in the low-amplitude case, the answer one gets depends strongly on where in the cycle one applies the perturbation. If one perturbs between consecutive spikes, where no cells

are firing, then the perturbation immediately triggers a new sequence of spikes, essentially indistinguishable from the original set except that they are translated uniformly in time For such perturbations one therefore finds a decorrelation time of zero. If, on the other hand, one perturbs near the top of a spike, where nearly all cells are firing, then one finds that the subsequent firing of the network is affected only for a few time steps, after which the original firing pattern is recovered exactly. One therefore concludes that the decorrelation time is infinite: the system is not decorrelated at all by the perturbation. Such discrepancies, obviously artifacts of the discrete variables in our model and the crudeness of our definition of the decorrelation time, do not occur in systems with continuous variables, where the computation of Lyapunov exponents is based on infinitesimal perturbations of the system

5. The infinite-size limit: coupled map model

The derivation of the infinite-size limit of the cellular automaton model of the CA3 region of the hippocampus relies on the absence of correlations in the inter-neuronal connections. The basic idea, familiar from statistical mechanics, is that in this limit one must keep track only of the average activity of each type of neuron, not of individual neurons. For example, knowing that a fraction $p(n)$ of all excitatory neurons fire at time n, one can calculate the probability distribution of excitatory inputs received by any given excitatory neuron at time $n+\tau_D^e$; (recall that τ_D^e is the time delay for a signal to propagate from one excitatory neuron to another). Similar knowledge of the distribution of inhibitory signals enables one to compute $p(n+1)$ from the firing rules described earlier Note that taking the thermodynamic limit requires an assumption about the way the number of outputs, z_e, z_f and z_s, from each cell of type e, f and s, respectively, scales with N. Since the surface area of the cell limits the number of inputs to it, and since the number of synapses per neuron in biological networks is typically quite insensitive to the size of the networ'k, we have decided to take z_e, z_f and z_s independent of N. This choice gives reasonable results in the limit of no inhibition ($K_f=K_s=0$; see the appendix), whereas allowing z_e, z_f and z_s to grow with N does not

In the appendix the derivation of two very simple $N\to\infty$ limits is presented in some detail, to make the general idea clear One of these is the case without inhibition, with a single refractory time, and no spontaneous firing or time delays, the other has inhibition, but a simple majority-rule firing algorithm. The complete infinite-size model, containing the three different types of neurons and the additional time variables describing the propagation delays, spontaneous firing times, duration of bursts and different refractory times, follows as a straightforward but tedious generalization of the procedure outlined for these elementary special cases. In this section we merely write the final equations down, and summarize the results of solving them on the computer.

In the finite-size model we used distributions of spontaneous firing times and refractory times However, the simulations of that model showed that, while it was important to use a distribution of spontaneous firing times, one could use a single refractory time without changing the results Since in the $N\to\infty$ models additional equations are required for every distinct value of τ_S and τ_R, it is most efficient to take just one refractory time. Thus the excitatory neurons will be divided into groups, labelled by the index k, which correspond to different spontaneous firing times τ_S^k, but a common refractory time τ_R.

The full model is then described by the following set of coupled equations

$$S_f(n+1) = \{1 - Y_f(n)\}\{1 - \exp(-z_e x_e(n))\}$$

$$Y_f(n+1) = \sum_{l=1}^{d_f - 1} S_f(n+2-l)$$

$$S_s(n+1) = \{1 - Y_s(n)\}\{1 - \exp(-z_e x_e(n))\}$$

$$Y_s(n+1) = \sum_{l=1}^{d_s - 1} S_s(n+2-l)$$

$$S_e^k(n) = \sum_{n'=n-d_e-\tau_S^k}^{n-d_e} V_e^k(n, n') P^k(n, n')$$

$$Y_e^k(n) = \sum_{l=1}^{d_e - 1} S_e^k(n+2-l)$$

Here $V_e^k(n, n')$ satisfies the recursion relation,

$$V_e^k(n+1, n') = V_e^k(n, n')\{1 - P^k(n, n')\}$$

and

$$P^k(n, n') \equiv \sum_{m_e=0}^{\infty} \sum_{m_f=0}^{\infty} \sum_{m_s=0}^{\infty} \{p(m_e, m_s, m_f; n)\theta(K_e m_e - K_f m_f - K_s m_s - h(n, n'))\}$$

for $(n - d_e - \tau_S^k) < n' < n$, with

$$p(m_e, m_f, m_s, n) = \exp\{-z_e w_e x_e(n - \tau_D^e) - z_f w_f x_f(n - \tau_D^f) - z_s w_s x_s(n - \tau_D^s)\}$$

$$\times (z_e w_e x_e(n - \tau_D^e))^{m_e} (z_f w_f x_f(n - \tau_D^f))^{m_f} (z_s w_s x_s(n - \tau_D^s))^{m_s} \frac{1}{m_e! m_f! m_s!}$$

(This equation is a straightforward generalization of equation (A2) in the appendix.) Here

$$w_e x_e(n) = \sum_k w_e^k x_e^k(n)$$

$$x_e^k(n) = S_e^k(n) + Y_e^k(n-1)$$

$$x_f(n) = S_f(n) + Y_f(n-1)$$

$$x_s(n) = S_s(n) + Y_s(n-1)$$

where in turn w_e^k is the fraction of neurons which are excitatory and have spontaneous firing time τ_S^k. Further, w_f, w_s denote the fractions of fast and slow inhibitory neurons, $w_e = \Sigma_k w_e^k$ is the total fraction of excitatory neurons, and $w_e + w_f + w_s = 1$, $x_e(n)$, $x_f(n)$, $x_s(n)$ denote the fractions of excitatory, fast, and slow inhibitory neurons which fire at n; recall that z_e, z_f, z_s are the numbers of excitatory, fast, and slow inhibitory outputs for each e, f, s neuron. $S_e^k(n)$, $S_f(n)$, $S_s(n)$ are the fractions of (e, k), f and s neurons which fire through stimulation or, for e neurons, spontaneously, at time n. $Y_e^k(n)$, $Y_f(n)$, $Y_s(n)$ are fractions of (e, k), f, s neurons which fire at $n+1$ simply because the duration of a burst is longer than one time step; d_e, d_f, d_s denote the durations of the bursts. $V_e^k(n, n')$ is the fraction of (e, k) neurons which last fired spontaneously or by stimulation at time n' and are available for firing at time n; (all are available except those already firing). $P(n, n')$ is the probability that such a neuron fires at time n. The function $h(n, n')$ denotes the firing threshold at time

n for e neurons which last fired at n' Specifically, we use

$$h(n, n') = \begin{cases} (F_0)(n - n' - \tau_R)/\tau_R & (n - n') < \tau_R \\ 0 & (n - n') > \tau_R \end{cases}$$

K_e, K_f, K_s are the strengths of the e, f, s connections, τ_D^e, τ_D^f, τ_D^s are the propagation delays for e, f, s neurons Finally $\theta(x)$ is the step function That is, for $n - n' > \tau_R$ an excitatory neuron will fire provided

$$K_e m_e > K_f m_f + K_s m_s$$

where m_e, m_f, m_s are the number of e, f, s inputs The inhibitory neurons will fire any time there is an excitatory input, $m_e > 0$, independent of the inhibitory inputs. Finally,

$$x(n) \equiv w_e x_e(n) + w_f x_f(n) + w_s x_s(n)$$

is the total fraction of neurons firing at n

In addition, the following boundary conditions must be satisfied

$$P^k(n, n - d_e - \tau_S^k) = 1$$

$$V_e^k(n, n - d_e) = S_e^k(n - d_e)$$

The first condition assures that an excitatory neuron in group k will fire spontaneously with unit probability at a time $d_e + \tau_S^k$ after the initiation of the previous burst, as required by the definition of τ_S^k The second condition follows directly from the definitions of V_e^k and S_e^k, and the definition of d_e as the duration of the burst of an excitatory neuron.

Direct numerical solution of these equations again yields a transition from a low-amplitude chaotic signal for $K_f = 10$ to a nearly periodic, large-amplitude, peaked structure for $K_f = 0$

Figures 3(*a*)–(*d*) show the behaviour of the average signal $x(n)$ for $K_f = 10$, $K_f = 0\,51251$, $K_f = 0\,51250$ and $K_f = 0$ The behaviour is remarkably similar to that obtained for the finite-size model, shown in figures 1(*a*)–(*d*), including the sharpness of the transition The main difference is that the peak amplitude of the high-amplitude phase is smaller in the infinite-size model

To save on computing time required to generate figures 3(*a*)–(*d*), we reduced the values of the various time constants by roughly a factor of 10 compared to those used in figures 1(*a*)–(*d*) The actual values used were as follows. $N_e/N = 0.9$, $N_s/N = N_f/N = 0\,05$, $z_e = 20$, $z_f = z_s = 200$, $d_e = 8$, $d_f = 2$, $d_s = 10$, $\tau_R = 80$, $\tau_D^e = 2$, $\tau_D^s = 6$, $F_0 = 1\,0$ and $\tau_S^k = 3\,33k$, $k = 0,\ \ldots, 12$. These same parameter values were then used to repeat the finite-size calculations for $N \leqslant 10\,000$ The behaviour was essentially unchanged from figures 1(*a*)–(*d*), except for a reduction by a factor of 10 of the overall time scale Also, little difference in behaviour was observed for $N = 900$ and $N = 10\,000$ so even systems of modest size behave as though close to the thermodynamic limit. This is consistent with the close agreement between figures 1 and 3 (Recall that $N = 900$ was used in generating figures 1(*a*)-(*d*))

The model contains a large number of parameters and by varying these a wide variety of behaviours can be obtained No attempt has been made to explore in detail this very large phase space We have so far concentrated on trying to reproduce experimentally observed behaviours using experimentally determined parameters.

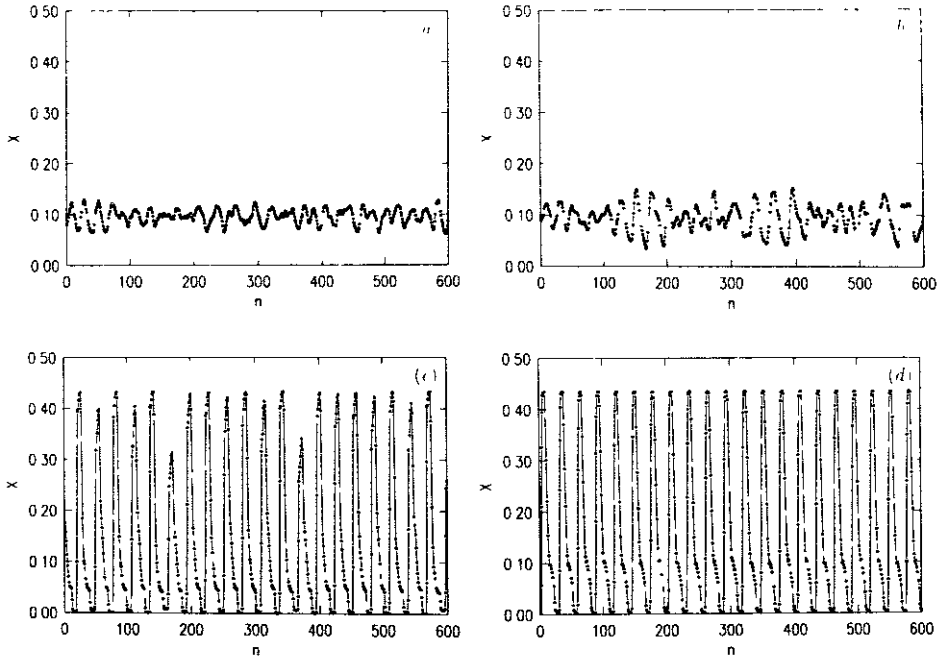

Figure 3. Fraction of neurons firing as a function of time for the infinite-size model (*a*) $K_f = 10$, (*b*) $K_f = 0.512\,51$ (*c*) $K_f = 0.512\,50$, (*d*) $K_f = 0$

6. Summary and outlook

In this paper we have summarized the construction and simulation of a model of the hippocampus (CA3) in which the neurons are represented by binary variables The connectivity of the network, propagation of signals through it, and firing rules are chosen to approximate the known biology reasonably faithfully Thus the parameters that specify the model are all taken from the results of experimental investigations. Our main finding is that the average activity of this simple cellular automaton model, both for finite-size samples with up to 10000 neurons and in the infinite-size limit, where the model reduces to a set of coupled maps, mimics rather closely that of real hippocampal slices and of the more realistic model from which our model derives. Though it is too early to be certain, this suggests that understanding the complex internal structure of neurons in the hippocampus may not be necessary for understanding certain aspects of its behaviour and function.

It is important to keep in mind that without knowing how the hippocampus works it is difficult to know how best to compare models with experiments. It is also quite likely that there are correlations in the firing patterns of the different neurons which are crucial to the function of the hippocampus but which are lost in a complete spatial average. A model such as the one discussed here may successfully reproduce the typical firing pattern of any one neuron, as well as the average activity, without capturing these

correlations Indeed, one could almost certainly reproduce the average activities discussed here with a single-variable nonlinear map with parameters to switch from low- to high-amplitude oscillations We have not tried to do this since sacrificing the identity of the individual neurons almost certainly means losing any serious contact with the biology The importance of spatio-temporal patterns of neuronal activity is so widespread in biological neural networks — sensory systems such as visual or auditory networks, motor networks (where successful function depends on particular motor neurons being driven with correct amplitude at specific times), and invertebrate central pattern generators (where the activity of particular neurons correlates with distinct aspects of behaviour) are but three examples — that we assume such patterns are likewise critical in the hippocampus In eliminating individual neurons, moreover, one loses contact with those experiments which study spatio-temporal correlations of firing rates of different neurons

The possibility of our model missing vital correlations between neurons looms particularly large in view of our choosing the connections from neuron to neuron randomly The real hippocampus presumably establishes, eliminates, or modifies connection strengths on the basis of its own activity and on inputs from other parts of the brain It seems probable that such 'learned' connections give rise to correlations in activity which a random network simply cannot generate Given our model's acceptable authenticity at the spatial average level, and its computational simplicity, we hope that it will help us explore such questions We are, for example, working on incorporating into it simple algorithms for long-term potentiation which are consistent with available experimental data (in collaboration with G Tesauro). By studying the distribution of connection strengths and the firing patterns that result, we anticipate building up an understanding of correlations in the model, and trying to match these with existing and future observations The ultimate goal, still remote at this stage, is to obtain insight into the computational capabilities of the hippocampus, and hence clues as to its function

Appendix

To illustrate the approach used in deriving the coupled map equations for the $N \to \infty$ limit, we consider first a simple model which contains only excitatory neurons with a single refractory time, τ_R. The model contains no spontaneous firing or propagation delays, the duration of a burst is one time step There is no firing during the refractory period ($F_0 = \infty$). Outside the refractory period, a single excitatory input is sufficient to make a neuron fire

Let $r_n = x_n N$ be the number of neurons firing at time n and let $q_n = y_n N$ be the number of neurons (other than the r_n firing ones) unavailable to fire at $n+1$, due to refractoriness If each neuron sends an output signal to precisely z other neurons, chosen randomly, then the number of neurons firing at time $n+1$ can be written as

$$r_{n+1} = (N - q_n - r_n)[1 - (1 - z/N)^{r_n}]$$

Here $(N - q_n - r_n)$ is the number of neurons available to fire. The second factor is the probability that each such neuron receives an input signal from one that fired at n The probability that a given neuron receives an input from any other neuron is, for large N, equal to z/N Thus $(1 - z/N)^{r_n}$ is the probability that a given neuron receives no signal from any of the r_n neurons that fired at n

The recursion relation for q_n takes the form

$$q_{n+1} = q_n + r_n - r_{n-\tau_R+1}$$

To q_n we add r_n, the number of those that fired at n which are, therefore, not available at $n+1$ because of the refractory time, and subtract $r_{n-\tau_R+1}$, the number of those that fired at $n-\tau_R+1$ which, therefore, become available to fire again at $n+1$. Taking the limit $N \to \infty$ we obtain two simple coupled nonlinear map equations

$$x_{n+1} = (1 - x_n - y_n)[1 - \exp(-zx_n)]$$

$$y_{n+1} = y_n + x_n - x_{n-\tau_R+1}.$$

Straightforward numerical study shows that as a function of the two parameters z and τ_R this simple model gives rise to a complex phase diagram consisting of domains of fixed points, cycles, and chaotic behaviour.

As a further illustration, we consider a model containing both excitatory and inhibitory neurons, with equal-strength inhibitory and excitatory connections and a simple majority firing rule $m_e > m_i$, where m_e (m_i) is the number of excitatory (inhibitory) inputs. The corresponding coupled map equations then take the form

$$x^e_{n+1} = (1 - x^e_n - y^e_n)P(x^e_n, x^i_n)$$

$$x^i_{n+1} = (1 - x^i_n - y^i_n)P(x^e_n, x^i_n)$$

$$y^e_{n+1} = y^e_n + x^e_n - x^e_{n-\tau^e_R+1}$$

$$y^i_{n+1} = y^i_n + x^i_n - x^i_{n-\tau^i_R+1}$$

where we have introduced different refractory times τ^e_R and τ^i_R for the excitatory and inhibitory neurons.

Here $P(x^e_n, x^i_n)$ denotes the probability that the inputs to a given neuron (either excitatory or inhibitory) at time $n+1$ satisfy the condition $m_e > m_i$.

$$P(x^e_n, x^i_n) = \sum_{m_e=1}^{\tilde{N}_e} \sum_{m_i=1}^{m_e-1} p(m_e)p(m_i).$$

Here $p(m_e)$ and $p(m_i)$ are the respective probabilities of having exactly m_e excitatory and m_i inhibitory inputs. The inner sum enforces the threshold condition $m_e > m_i$, and

$$\tilde{N}_e = x^e_n N_e = x^e_n w_e N$$

is the total number of excitatory neurons firing at n, where w_e is the fraction of neurons which are excitatory. The probability of a given neuron having exactly m_e inputs from excitatory neurons that fired at n is

$$p(m_e) = \binom{\tilde{N}_e}{m_e}\left(\frac{z_e}{N}\right)^{m_e}\left(1 - \frac{z_e}{N}\right)^{\tilde{N}_e - m_e} \tag{A1}$$

where the first factor selects m_e neurons out of the total number of excitatory neurons, $\tilde{N}_e$, that fired at n. The second factor is the probability that each of these sends an output to the given neuron; the last factor is the probability that none of the other neurons that fired at n is connected to the given neuron, in order to ensure exactly m_e inputs. In the limit $N \to \infty$, this expression reduces to

$$p(m_e) = (x^e_n w_e z_e)^{m_e} \exp(-z_e w_e x^e_n)/m_e! \tag{A2}$$

The expression for $p(m_i)$ has the identical form with e everywhere replaced by i (note that

$w_i = 1 - w_e$). As a function of the parameters τ_e, τ_i, τ_R^e, τ_R^i and w_e, a very complex phase diagram including regions of fixed points, cycles and chaotic behaviour is obtained. Chaotic behaviour occurs most commonly, though often the chaotic trajectories are very nearly periodic.

References

Alonso A, Gaztelu J M, Buño W Jr and García-Austt E 1987 Cross-correlation analysis of septohippocampal neurons during θ-rhythm *Brain Res.* **413** 135–46

Amit D J 1989 *Modelling Brain Function. The world of attractor neural networks* (Cambridge: Cambridge University Press)

Boss B D, Turlejski K, Stanfield B B and Cowan W M 1987 On the numbers of neurons in fields CA1 and CA3 of the hippocampus of Sprague–Dawley and Wistar rats *Brain Res.* **406** 280–7

Brown M W and Cassell M D 1980 Estimates of the number of neurons in the human hippocampus *J. Physiol.* **301** 58P–59P

Buzsáki G 1986 Hippocampal sharp waves: their origin and significance *Brain Res.* **398** 242–52

Buzsáki G, Leung L-W S and Vanderwolf C H 1983 Cellular bases of hippocampal EEG in the behaving rat *Brain Res. Rev.* **6** 139–71

Chan-Palay V and Kohler C (ed) 1989 *The Hippocampus: New Vistas* (New York: Alan Liss)

Collet P and Eckmann J-P 1980 *Iterated Maps on the Interval as Dynamical Systems* (Basel: Birkhauser)

Collingridge G L, Gage P W and Robertson B 1984 Inhibitory post-synaptic currents in rat hippocampal CA1 neurones *J. Physiol.* **356** 551–64

Daly D D 1990 Epilepsy and syncope *Current Practice of Clinical Electroencephalography* ed D D Daly and T A Pedley (New York: Raven) 2nd edn pp 269–334

Eichenbaum H and Cohen N J 1988 Representation in the hippocampus: what do hippocampal neurons code? *Trends Neurosci.* **11** 244–8

Frotscher M, Kugler P, Misgeld U and Zilles K 1988 *Neurotransmission in the Hippocampus* (Berlin: Springer)

Gastaut H 1970 Clinical and electroencephalographical classification of epileptic seizures *Epilepsia* **11** 102–13

Getting P A and Dekin M S 1985 Mechanisms of pattern generation underlying swimming in *Tritonia* IV. Gating of central pattern generator *J. Neurophysiol.* **53** 466–80

Green J D and Arduini A A 1954 Hippocampal electrical activity in arousal *J. Neurophysiol.* **17** 533–57

Hablitz J J and Thalmann R H 1987 Conductance changes underlying a late synaptic hyperpolarization in hippocampal CA3 neurons *J. Neurophysiol.* **58** 160–79

Heinzel H-G 1988a Gastric mill activity in the lobster I. Spontaneous modes of chewing *J. Neurophysiol.* **59** 528–50

—— 1988b Gastric mill activity in the lobster II. Proctolin and octopamine initiate and modulate chewing *J. Neurophysiol.* **59** 551–65

Heinzel H-G and Selverston A I 1988 Gastric mill activity in the lobster III. Effects of proctolin on the isolated central pattern generator *J. Neurophysiol.* **59** 566–85

Kass I S and Lipton P 1982 Mechanisms involved in irreversible anoxic damage to the in vitro rat hippocampal slice *J. Physiol.* **332** 459–72

Meldrum B S, Evans M C, Swan J H and Simon R P 1987 Protection against hypoxic/ischaemic brain damage with excitatory amino acid antagonists *Med. Biol.* **65** 153–7

Miles R 1990 Synaptic excitation of inhibitory cells by single CA3 hippocampal pyramidal cells of the guinea-pig in vitro *J. Physiol.* **428** 61–77

Miles R, Traub R D and Wong R K S 1988 Spread of synchronous firing in longitudinal slices from the CA3 region of the hippocampus *J. Neurophysiol.* **60** 1481–96

Miles R and Wong R K S 1984 Unitary inhibitory synaptic potentials in the guinea-pig hippocampus in vitro *J. Physiol.* **356** 97–113

—— 1986 Excitatory synaptic interactions between CA3 neurones in the guinea-pig hippocampus *J. Physiol.* **373** 397–418

—— 1987 Inhibitory control of local excitatory circuits in the guinea-pig hippocampus *J. Physiol.* **388** 611–29

Muller R U and Kubie J L 1987 The effects of changes in the environment on the spatial firing of hippocampal complex-spike cells *J. Neurosci.* **7** 1951–68

Muller R U, Kubie J L and Ranck J B Jr 1987 Spatial firing patterns of hippocampal complex-spike cells in a fixed environment *J. Neurosci.* **7** 1935–50

O'Keefe J and Nadel L 1978 *The Hippocampus as a Cognitive Map* (Oxford: Clarendon Press)

Olney J W, Collins R C and Sloviter R S 1986 Excitotoxic mechanisms of epileptic brain damage *Advances in Neurology* vol 44 *Basic Mechanisms of the Epilepsies: Molecular and Cellular Approaches* ed A V Delgado-Escueta *et al* (New York: Raven Press) pp 857–77

Petsche H, Stumpf C and Gogolak G 1962 Significance of the rabbit's septum as a relay station between the midbrain and the hippocampus: I. The control of hippocampus arousal activity by septum cells *Electroenceph. Clin. Neurophysiol.* **14** 202–11

Rumelhart D E, McClelland J L and the PDP Research Group 1988 *Parallel Distributed Processing: Exploration in the Microstructure of Cognition, vol 1: Foundations; vol 2: Psychological and Biological Models* (Cambridge, MA: MIT Press)

Schneiderman J H 1986 Low concentrations of penicillin reveal rhythmic synchronous synaptic potentials in hippocampal slice *Brain Res.* **398** 231–41

Schwartzkroin P A and Haglund M M 1986 Spontaneous rhythmic synchronous activity in epileptic human and normal monkey temporal lobe *Epilepsia* **27** 523–33

Scoville W B and Milner B 1957 Loss of recent memory after bilateral hippocampal lesions *J. Neurol. Neurosurg. Psychiat.* **20** 11–21

Sloviter R S 1983 "Epileptic" brain damage in rats induced by sustained electrical stimulation of the perforant path: I. Acute electrophysiological and light microscopic studies *Brain Res. Bull.* **10** 675–97

Squire L R, Shimamura A P and Amaral D G 1989 Memory and the hippocampus *Neural Models of Plasticity* ed J H Byrne and W O Berry (San Diego: Academic Press) pp 208–39

Stewart M and Fox S E 1989 Two populations of rhythmically bursting neurons in rat medial septum are revealed by atropine *J. Neurophysiol.* **61** 982–93

Traub R D 1982 Simulation of intrinsic bursting in CA3 hippocampal neurons *Neuroscience* **7** 1233–42

Traub R D and Miles R 1991 *Neuronal Networks of the Hippocampus* (Cambridge: Cambridge University Press)

Traub R D, Miles R and Wong R K S 1987a Models of synchronized hippocampal bursts in the presence of inhibition: I. Single population events *J. Neurophysiol.* **58** 739–51

—— 1989 Model of the origin of rhythmic population oscillations in the hippocampal slice *Science* **243** 1319–25

Traub R D, Miles R, Wong R K S, Schulman L S and Schneiderman J H 1987b Models of synchronized hippocampal bursts in the presence of inhibition: II. Ongoing spontaneous population events *J. Neurophysiol.* **58** 752–64

Traub R D and Wong R K S 1982 Cellular mechanism of neuronal synchronization in epilepsy *Science* **216** 745–7

Vanderwolf C H 1969 Hippocampal electrical activity and voluntary movement in the rat *Electroenceph. Clin. Neurophysiol.* **26** 407–18

Wong R K S and Prince D A 1981 Afterpotential generation in hippocampal pyramidal cells *J. Neurophysiol.* **45** 86–97

Zola-Morgan S, Squire L R and Amaral D G 1986 Human amnesia and the medial temporal region: enduring memory impairment following a bilateral lesion limited to field CA1 of the hippocampus *J. Neurosci.* **6** 2950–67